

Topology of the $O(3)$ non-linear sigma model under the gradient flow

Stuart Thomas^{a,*} and Christopher Monahan^{a,b}

^a*Department of Physics, William & Mary,
300 Ukrop Way, Williamsburg, VA, USA*

^b*Thomas Jefferson National Accelerator Facility,
12000 Jefferson Avenue, Newport News, VA, USA*

E-mail: snthomas01@email.wm.edu, cjmonahan@wm.edu

The $O(3)$ non-linear sigma model (NLSM) is a prototypical field theory for QCD and ferromagnetism, featuring topological qualities. Though the topological susceptibility χ_t should vanish in physical theories, lattice simulations of the NLSM find that χ_t diverges in the continuum limit. We study the effect of the gradient flow on this quantity using a Markov Chain Monte Carlo method, finding that a logarithmic divergence persists. This result supports a previous study and indicates that either the definition of topological charge is problematic or the NLSM has no well-defined continuum limit. We also introduce a θ -term and analyze the topological charge as a function of θ under the gradient flow.

*The 38th International Symposium on Lattice Field Theory, LATTICE2021 26th-30th July, 2021
Zoom/Gather@Massachusetts Institute of Technology*

*Speaker

1. Introduction

Spin models provide a framework for understanding the physics of strongly-coupled systems, from solid state and condensed matter systems to nuclear and particle physics. The non-linear sigma model (NLSM), in particular, has provided a rich arena in which to study nonperturbative effects. In solid-state systems, this model describes Heisenberg ferromagnets [1] and in nuclear physics, it acts as a prototype for quantum chromodynamics (QCD), the gauge theory of the strong nuclear force. In general, the NLSM shares key features with non-Abelian gauge theories such as QCD, including a mass gap and asymptotic freedom [2], and has proved a useful model for exploring the effect of these properties in a simpler system.

We consider the $O(3)$ NLSM in 1+1 dimensions (one dimension of space, one dimension of time). This theory exhibits topological properties, such as *instantons*, or classical field solutions at local minima of the action in Euclidean space. These topologically protected solutions cannot evolve into the vacuum state via local fluctuations. This property has become critically important to quantum field theories in cosmology and high energy physics [3]. *CJM: Can we provide a more explicit example(s) here? Statement is very vague at the moment.* Additionally, topological stability may become a key tool for fault-tolerant quantum computers [4]. In these devices, topology protects the delicate quantum states necessary for information processing.

The protection of topological instantons in the 1+1 $O(3)$ NLSM relies on a vanishing topological susceptibility. However, the convergence of this quantity is still unknown. [5] While the some analytical arguments argue the topological susceptibility should approach zero in the continuum limit, numerical results on the lattice predict infinities [6]. In an attempt to shed light on this contradiction, we apply the gradient flow, a local smearing of operators which preserves gauge invariance. In quantum chromodynamics, this technique has corroborated a previous analytical result [7] by removing ultraviolet divergences on the lattice [8]. This success has motivated the gradient flow to calculate the topological susceptibility in the 1+1 $O(3)$ NLSM. Despite this intuition, recent studies demonstrate that the observable still diverges in the continuum limit [5].

We also study a second perspective on the topological susceptibility arising from the introduction of a θ -term into the field Lagrangian. This term drives the vacuum state into a topological phase [9]. Differentiating the field's partition function with respect to θ yields a value proportional to the topological susceptibility. The effect of nonzero θ on the theory therefore should reflect the divergence in the continuum limit. In this work we verify the divergence of the topological susceptibility and develop a clearer picture of how the θ -term affects the topology of the 1+1 $O(3)$ NLSM.

To numerically study the topological qualities of the NLSM, we first implement a Markov chain Monte Carlo simulation using Metropolis and Wolff cluster [10] algorithms. Since the gradient flow has no exact solution in the NLSM we implement a numerical solution using a fourth-order Runge-Kutta approximation with automatic step sizing. By applying the gradient flow to every configuration in the sample, we can measure its effect on the topological charge and susceptibility.

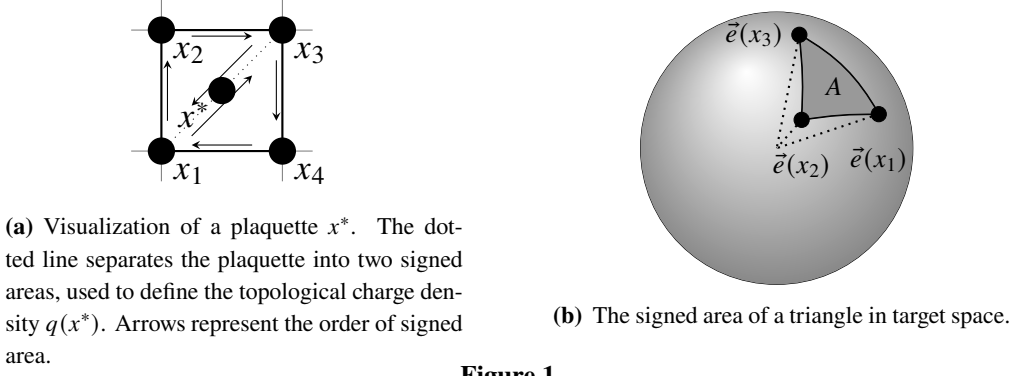


Figure 1

2. The Non-Linear Sigma Model

We study the $O(3)$ NLSM in two dimensions **CJM: [In Euclidean space it does not really make sense to distinguish time and space, unless we start in Minkowski spacetime and then Wick rotate.]**, defined by the Euclidean action

$$S_E = \frac{\beta}{2} \int d^2x \sum_{i=1}^2 (\partial_i \vec{e})^2,$$

where \vec{e} is 3-component real vector constrained by $|\vec{e}| = 1$ and β is the inverse coupling constant. Following [6], we define the topological charge density, $q(x^*)$, for each plaquette x^* such that the total topological charge is

$$Q = \sum_{x^*} q(x^*), \quad (1)$$

where

$$q(x^*) = \frac{1}{4\pi} \left[A(\vec{e}(x_1), \vec{e}(x_2), \vec{e}(x_3)) + A(\vec{e}(x_1), \vec{e}(x_3), \vec{e}(x_4)) \right]. \quad (2)$$

Here, A is the signed area of the triangle in target space, which we represent in the left-hand figure of Fig. 1b. This value is defined if $A \neq 0, 2\pi$, or in other words, as long as the three points on the sphere are distinct and do not form a hemisphere. In numerical calculations, these points can be ignored. Therefore, we impose that the signed area is defined on the smallest spherical triangle, or $-2\pi < A < 2\pi$.

We define the topological susceptibility χ_t

$$\chi_t \equiv \frac{1}{L^2} (\langle Q^2 \rangle - \langle Q \rangle^2). \quad (3)$$

In the trivial case, $\langle Q \rangle$ is equal to 0 and on this lattice, this becomes

$$\chi_t = \frac{1}{L^2} \sum_{x^*, y^*} \langle q(x^*) q(y^*) \rangle = \frac{1}{L^2} \sum_{x^*} \langle q(x^*) q(0) \rangle, \quad (4)$$

where in the second equality we have assumed periodic boundary conditions. The topological susceptibility diverges in the continuum limit owing solely to the $x^* = 0$ term [5]. This divergence exists in QCD as well [8].

Additionally, we can generalize the NLSM to have a nonzero vacuum expectation value for the topological charge, manifested by the addition of a “ θ -term”:

$$S[\vec{e}] \rightarrow S[\vec{e}] - i\theta Q[\vec{e}].$$

defining the “nontrivial” NLSM. We find that the topological susceptibility in the trivial case depends on the charge in the nontrivial model:

$$\chi_t \propto \left. \frac{d \operatorname{Im}\langle Q \rangle}{d\theta} \right|_{\theta=0} \quad (5)$$

2.1 Gradient flow

CJM: Sentences/paragraph introducing continuous gradient flow here

3. Numerical implementation

We implement a numerical Monte Carlo method to study the NLSM in two dimensions using the discretized action

$$S_{\text{lat}}[\vec{e}] = \sum_i \left[2 - \vec{e}(x + a\hat{t}) \cdot \vec{e}(x) - \vec{e}(x + a\hat{x}) \cdot \vec{e}(x) \right]. \quad (6)$$

We generate configurations using the Metropolis [] and Wolff cluster [10] algorithms, implemented in C++ and parallelized through the Message Passing Interface with a checkerboard algorithm [].

We thermalize the configurations with 1000 sweeps, with a cluster update every five sweeps, and illustrate a sample Markov chain in Fig. 2, where we plot the action as a function of Metropolis sweeps. We use Wolff’s automatic windowing procedure [11] to estimate the autocorrelation times for various observables, such as the magnetic susceptibility χ_m . We measure observables every 50 sweeps for each simulation.

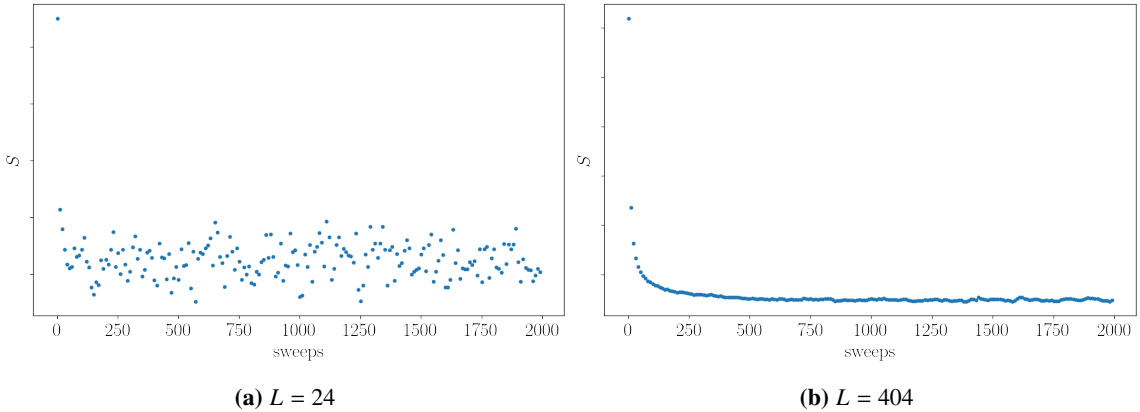


Figure 2: Plots of the action as a function of Monte Carlo time, starting with a random NLSM lattice.

We apply the gradient flow equation

$$\partial_\tau \vec{e}(\tau, x) = \left(1 - \vec{e}(\tau, x) \vec{e}(\tau, x)^T \right) \partial^2 \vec{e}(\tau, x), \quad (7)$$

where the Laplacian operator ∂^2 is defined as

$$\partial^2 \vec{e}(\tau, x) = \vec{e}(\tau, x + a\hat{t}) + \vec{e}(\tau, x - a\hat{t}) + \vec{e}(\tau, x + a\hat{x}) + \vec{e}(\tau, x - a\hat{x}) - 4\vec{e}(\tau, x).$$

We numerically solve the ordinary differential equation in Eq. 7 using a fourth-order Runge-Kutta approximation. To increase the efficiency of this algorithm, we implement the step-doubling algorithm to adaptively adjust the step size. If the error of a Runge-Kutta step is greater than the tolerance, the same step is repeated with half the step size. Alternatively, if the error is less than half of the tolerance, the step size is doubled for the next calculation. Finally, if the step size is greater than the distance to the next measurement, that distance is used as the step size, using the normal value afterwards. Otherwise, the algorithm proceeds with the consistent step size.

To calculate the error, we compare one lattice \vec{e}_1 produced using a step of size $2h$ with another lattice \vec{e}_2 produced via two steps of size h . The error Δ can be estimated to up the fifth order of h as [12]

$$\Delta = \frac{1}{15} \sqrt{\sum_x |\vec{e}_2(x) - \vec{e}_1(x)|} \quad (8)$$

The tolerance used in this work is $\Delta_{max} = 0.01$.

4. Results

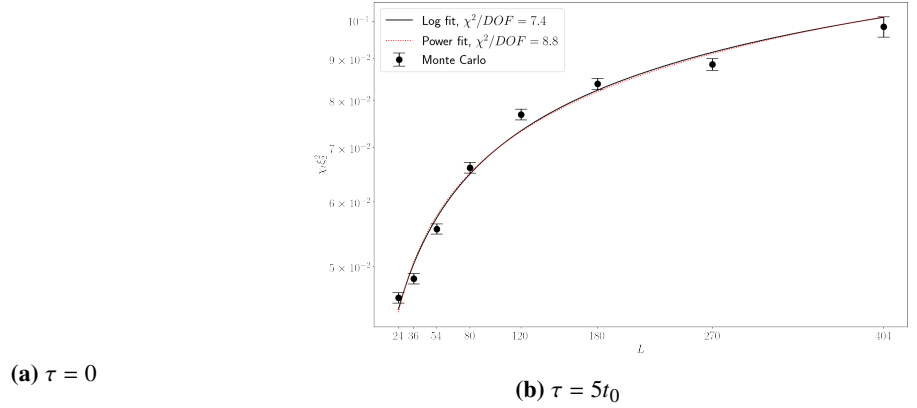


Figure 3: $\chi_t \xi_2^2$ as a function of L . ξ_2 is the second moment of the correlation function and t_0 is a scale-independent unit of flow time. We fit the data with both a logarithmic and power fit. Simulation run with 10,000 measurements every 50 sweeps, 1,000 sweep thermalization. In the $\tau = 0$ case, we have compared our result with the curve fits found in [5].

References

- [1] C. Callan, D. Friedan, E. Martinec and M. Perry, *Strings in background fields*, .
- [2] A. Polyakov, *Interaction of goldstone particles in two dimensions. Applications to ferromagnets and massive Yang-Mills fields*, .

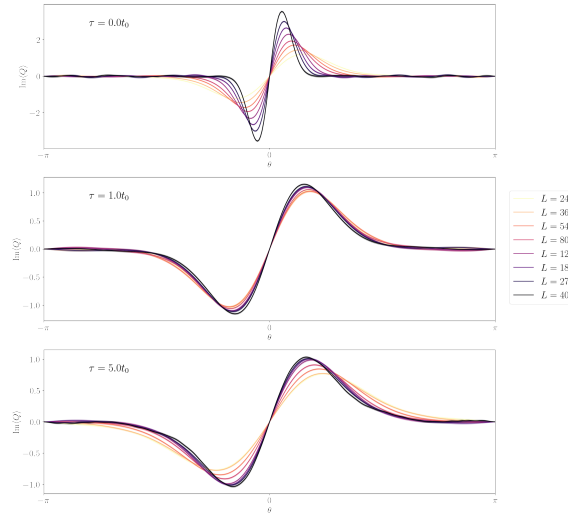


Figure 4: Nontrivial $\text{Im}\langle Q \rangle$ as a function of θ . Simulation run with 10,000 measurements, every 50 sweeps, 1,000 sweep thermalization. Note the different scaling of the y-axis.

- [3] P. Goddard and P. Mansfield, *Topological structures in field theories*, .
- [4] A.Y. Kitaev, *Quantum computations: Algorithms and error correction*, .
- [5] W. Bietenholz, P. de Forcrand, U. Gerber, H. Mejía-Díaz and I.O. Sandoval, *Topological Susceptibility of the 2d $O(3)$ Model under Gradient Flow*, [1808.08129](#).
- [6] B. Berg and M. Lüscher, *Definition and statistical distributions of a topological number in the lattice $O(3)$ σ -model*, .
- [7] L. Giusti, G. Rossi and M. Testa, *Topological susceptibility in full QCD with Ginsparg–Wilson fermions*, .
- [8] M. Bruno, S. Schaefer, R. Sommer and ALPHA Collaboration, *Topological susceptibility and the sampling of field space in $N_f = 2$ lattice QCD simulations*, .
- [9] B. Alles Salom and A. Papa, *Numerical Study of the mass spectrum in the 2D $O(3)$ sigma model with a theta term*, in *Proceedings of The XXV International Symposium on Lattice Field Theory — PoS(LATTICE 2007)*, p. 287, Sissa Medialab, [DOI](#).
- [10] U. Wolff, *Collective monte carlo updating for spin systems*, .
- [11] U. Wolff, *Monte Carlo errors with less errors*, [hep-lat/0306017](#).
- [12] W.T. Vetterling, W.H. Press, S.A. Teukolsky and B.P. Flannery, *Numerical Recipes: Example Book C*, Cambridge University Press.